Lattice Vibration Spectra. LXX. Evaluation of IR Reflection Spectra. Model Calculations and Experimental Data of $MnCr_2O_4$ Single Crystals

J. Himmrich, G. Schneider, J. Zwinscher, and H. D. Lutz
Universität Siegen, Anorganische Chemie I, Siegen, BRD

Z. Naturforsch. **46 a**, 1095–1102 (1991); received September 6, 1991

The various evaluation procedures of IR reflection spectra, viz. Kramer-Kronig analyses (KKA), 3 parameter (ω_{TO}, ϱ, γ) (3 PM), and 4 parameter (ω_{TO}, ω_{LO}, γ_{TO}, γ_{LO}) oscillator-model calculations (4 PM), are compared. For the zone-centre phonon energies, the oscillator parameters ω_{TO} and ω_{LO} of 4 PM as well as the frequencies of the dielectric functions ε'' and $-\mathrm{Im}(1/\hat{\varepsilon})$, respectively (KKA, 3 PM), are recommended. The pole frequencies of the $|\hat{\varepsilon}|$ functions yield too large TO/LO splittings, especially in the case of large damping of the phonons. In the case of asymmetric reststrahlen bands, the use of 4 PM with different damping constants γ for the TO and LO phonons is recommended. Computer simulations of the influence of the various oscillator parameters on the reflection spectra as well as the phonon frequencies of spinel-type $MnCr_2O_4$ are included.

Key words: Kramer-Kronig analyses; Oscillator-fit calculations, 3 Parameter and 4 parameter model; Phonon frequencies, Evaluation; Reststrahlen bands, Computer simulations; Spinel-type $MnCr_2O_4$.

1. Introduction

IR reflection spectra at near normal incidence are a valuable tool for determining the transversal (ω_{TO}) and longitudinal optical (ω_{LO}) zone-centre phonon frequencies of solids [1, 2]. There are two common procedures of evaluating the obtained spectra, viz. Kramers-Kronig analyses (KKA) [2–6] and the oscillator-fit methods (OF) [1, 7–15]. As a result of both Kramers-Kronig analyses and oscillator fits the dielectric (ε', ε'') and optic constants (n, k) as well as their frequency dependence (dispersion functions) are obtained. For calculating the phonon frequencies ω_{TO} and ω_{LO} there are various methods possible (see Table 1).

In this paper, we critically compare and discuss the various evaluation procedures of IR reflection spectra of single crystals (and pressed pellets in the case of cubic compounds). Furthermore, the influence of the various oscillator parameters on the reflection spectra are illustrated by computer simulations. To confirm our discussion of the evaluation procedures the results of spinel-type $MnCr_2O_4$ (single crystal) additional to those reported in [16] are given. For experimental details of recording IR reflection spectra and problems involved see [16–18].

Reprint requests to Prof. Dr. H. D. Lutz, Anorganische Chemie I, Universität-GH, W-5900 Siegen.

2. Evaluation of IR Reflection Spectra

The relations between the (observable) reflectivity R of a crystal face at near normal incidence and the dielectric and optic constants n, k, ε', and ε'' are given by the Fresnel equations

$$R = \frac{\hat{\varepsilon}^{1/2}-1}{\hat{\varepsilon}^{1/2}+1} = \frac{1+|\hat{\varepsilon}|-[(2(\varepsilon'+|\hat{\varepsilon}|]^{1/2}}{1+|\hat{\varepsilon}|+[2(\varepsilon'+|\hat{\varepsilon}|]^{1/2}}, \quad (1)$$

$$R = \frac{(n-1)^2+k^2}{(n+1)^2+k^2}, \quad (2)$$

$$|\hat{\varepsilon}| = (\varepsilon'^2+\varepsilon''^2)^{1/2}, \quad (3)$$

$$n = \{\tfrac{1}{2}[\varepsilon'+|\hat{\varepsilon}|]\}^{1/2}, \quad (4)$$

$$k = \varepsilon''/2n, \quad \text{and} \quad (5)$$

$$\varepsilon' = n^2+k^2 \quad (6)$$

with ε' and ε'' the real and imaginary part of the complex dielectric constant $\hat{\varepsilon}$ (permittivity), respectively, n the refractive index, and k the absorption index.

3. Kramers-Kronig Analysis

The Kramers-Kronig analysis (KKA) is based on the phase displacement $\theta_r(\omega')$ between incident and

0932-0784 / 91 / 1200-1095 $ 01.30/0. – Please order a reprint rather than making your own copy.

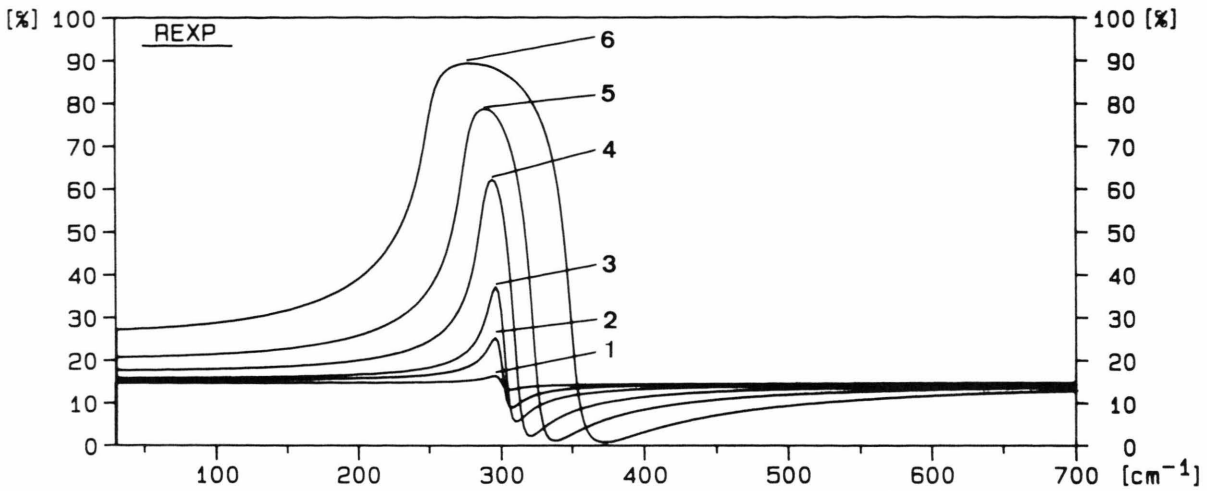

Fig. 1. Effect of increasing TO/LO splittings (1–6) on intensity and shape of a reststrahlen band with other oscillator parameters being constant ($\gamma = 10\ \mathrm{cm}^{-1}$, $\varepsilon_\infty = 5$) (1: $\omega_{TO} = 299.5$, $\omega_{LO} = 300.5\ \mathrm{cm}^{-1}$, 6: 250 and $350\ \mathrm{cm}^{-1}$) [22].

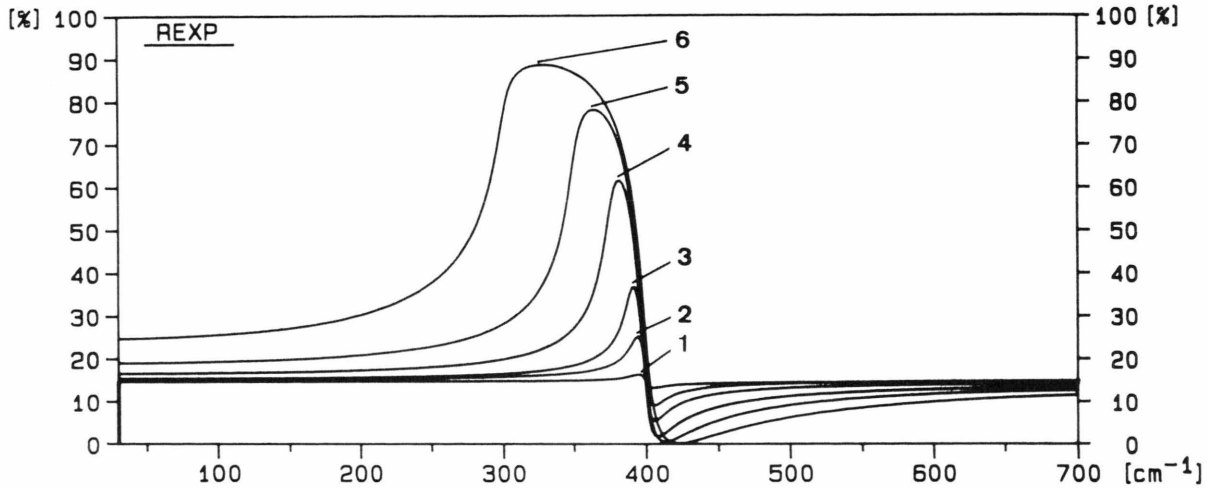

Fig. 2. Influence of ω_{TO} on position and shape of a reststrahlen band ($\omega_{LO} = 400\ \mathrm{cm}^{-1}$, $\gamma = 10\ \mathrm{cm}^{-1}$, $\varepsilon_\infty = 5$) (1: $\omega_{TO} = 399\ \mathrm{cm}^{-1}$, 6: $300\ \mathrm{cm}^{-1}$ [22].

reflected radiation, viz.

$$\theta_r(\omega') = \frac{2\omega'}{\pi} \int_0^\infty \frac{\ln r(\omega) - \ln r(\omega')}{\omega^2 - \omega'^2}\, \mathrm{d}\omega \qquad (7)$$

with r the reflectivity ($= \sqrt{R}$) and ω' and ω the frequency of θ_r and the running frequency, respectively. Equation (7) is commonly solved by the approximation of Roessler [5]. The optic constants can then be calculated by the equations

$$n(\omega') = \frac{1 - r(\omega')^2}{1 + r(\omega')^2 - 2r(\omega')\cos\theta_r(\omega')} \qquad (8)$$

and

$$k(\omega') = \frac{-2r(\omega')\sin\theta_r(\omega')}{1 + r(\omega')^2 - 2r(\omega')\cos\theta_r(\omega')} \qquad (9)$$

and, hence, the dielectric constants via (5) and (6).

The main advantage of Kramers-Kronig analysis is that no oscillator model must be used, i.e. knowledge of number and approximate frequencies of the phonon modes is not necessary. Disadvantages are that no separation of electronic, phononic, and plasmonic contributions to the dielectric function is possible and that the poles of the dispersion functions are less pronounced (owing to errors in determining the

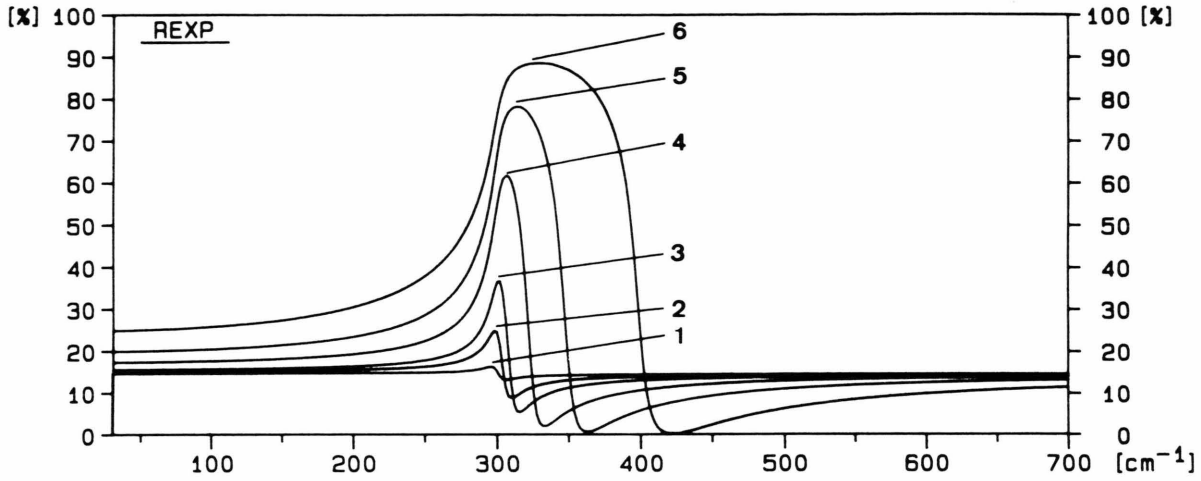

Fig. 3. Influence of ω_{LO} on position and shape of a reststrahlen band ($\omega_{TO} = 300\ cm^{-1}$, $\gamma = 10\ cm^{-1}$, $\varepsilon_\infty = 5$) (1: $\omega_{LO} = 301\ cm^{-1}$, 6: $400\ cm^{-1}$ [22].

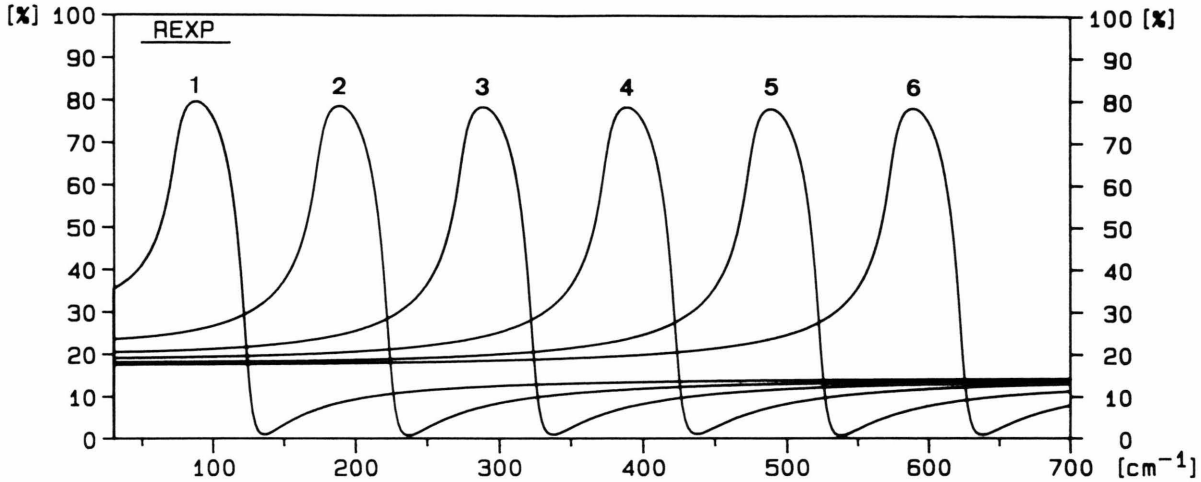

Fig. 4. Effect of increasing oscillator energy (1–6) on the shape of a reststrahlen band with TO/LO splitting being constant (TO/LO splitting = $50\ cm^{-1}$, $\gamma = 10\ cm^{-1}$, $\varepsilon_\infty = 5$) (1: $\omega_{TO} = 75\ cm^{-1}$, 6: $575\ cm^{-1}$) [22].

phase displacement θ_r). Therefore, the frequencies of low-intensity phonons sometimes cannot be obtained. If free-carrier contributions are present, only the frequencies of coupled plasmon-phonon states but not those of the pure LO phonon modes can be calculated [19, 20]. However, if the number of phonon modes present is not known, Kramers-Kronig analysis is the only evaluation procedure that can be used [16].

4. Oscillator-fit Calculation – 3 Parameter Model

The classical dielectric function originates from Huang [1]. It has been extended by Merten [10, 11] to polyatomic and anisotropic crystals. In the case of the classical oscillator-fit method (3 PM), the reflectivity R is fitted by suitable choice of the oscillator parameters ω_{TO}, ϱ, γ and ε_∞ (i.e. the phonon frequencies, the oscillator strengths, the damping constants, and the high-frequency dielectric constant, respectively) using the Fresnel equations given above and the classical dielectric sum-function

$$\hat{\varepsilon}_a(\omega) = \varepsilon_{\infty a} + \sum_{f=1}^{m_a} \frac{4\pi \varrho_{af}\, \omega_{TO\,af}^2}{\omega_{TO\,af}^2 - \omega^2 - i\gamma_{af}}, \tag{10}$$

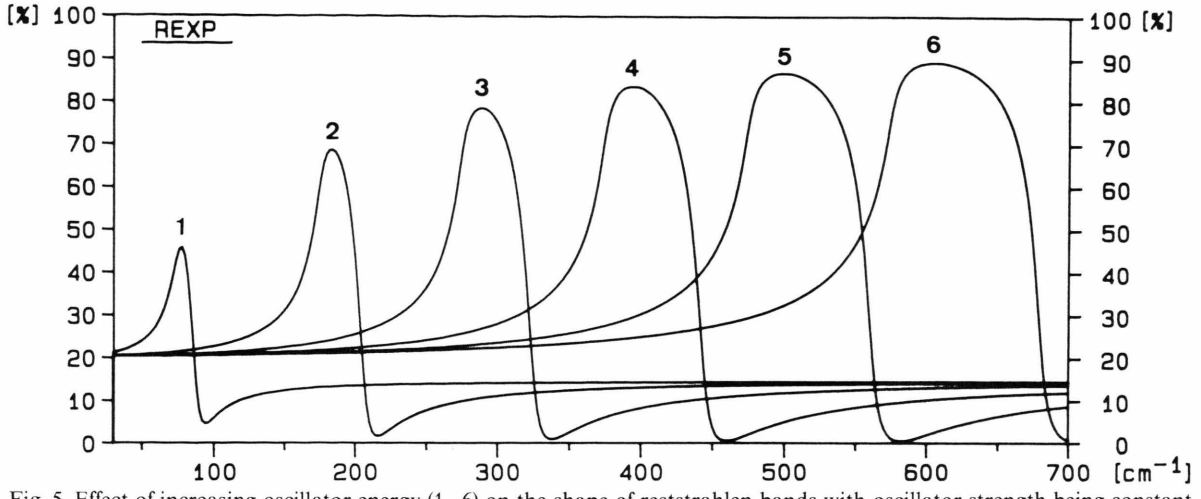

Fig. 5. Effect of increasing oscillator energy (1–6) on the shape of reststrahlen bands with oscillator strength being constant ($4\pi\varrho = 1.9835$, $\gamma = 10\ \mathrm{cm}^{-1}$, $\varepsilon_\infty = 5$) (1: $\omega_{TO} = 75$, $\omega_{LO} = 88.6\ \mathrm{cm}^{-1}$, 6: 575 and 679.5 cm^{-1}) [22].

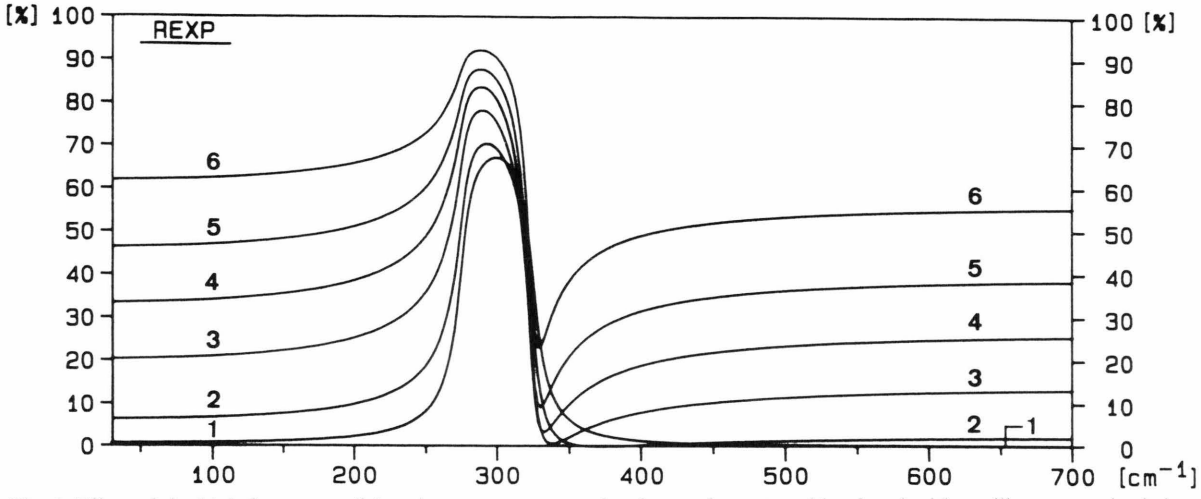

Fig. 6. Effect of the high-frequency dielectric constant ε_∞ on the shape of a reststrahlen band with oscillator energies being constant ($\omega_{TO} = 275\ \mathrm{cm}^{-1}$, $\omega_{LO} = 325\ \mathrm{cm}^{-1}$, $\gamma = 10\ \mathrm{cm}^{-1}$) (1: $\varepsilon^\infty = 1$, 6: 50) [22].

where a refers to one of the three IR-allowed species and f to the various oscillators (phonon modes). For details see [21, 22].

In the case of oscillator-fit calculations, the knowledge of the true number of IR active oscillators is necessary. However, the knowledge of the oscillator parameters is useful for the interpretation of the spectra obtained. Furthermore, plasmonic parts of the dielectric constant can be considered by an additional Drude term [19–23]

$$\hat{\varepsilon}_{pa}(\omega) = \frac{\varepsilon_{\infty a}\,\omega_{pa}^2}{\omega^2 - i\gamma_a\omega}. \tag{11}$$

Disadvantages are that (i) only ω_{TOaf}, but not ω_{LOaf} are obtained as oscillator parameters, (ii) the damping constants γ_{af} are regarded as equal for corresponding TO and LO phonons, which is not true, especially in the case of large TO/LO splittings as it is shown by the asymmetric shape of such reststrahlen bands, and (iii) the fit of the observed spectra is more complicated than it is with the 4 parameter model (see below).

5. Oscillator-fit Calculation – 4 Parameter Model

With this more recently [12–15] developed oscillator-fit (4 PM) procedure the oscillator parameters

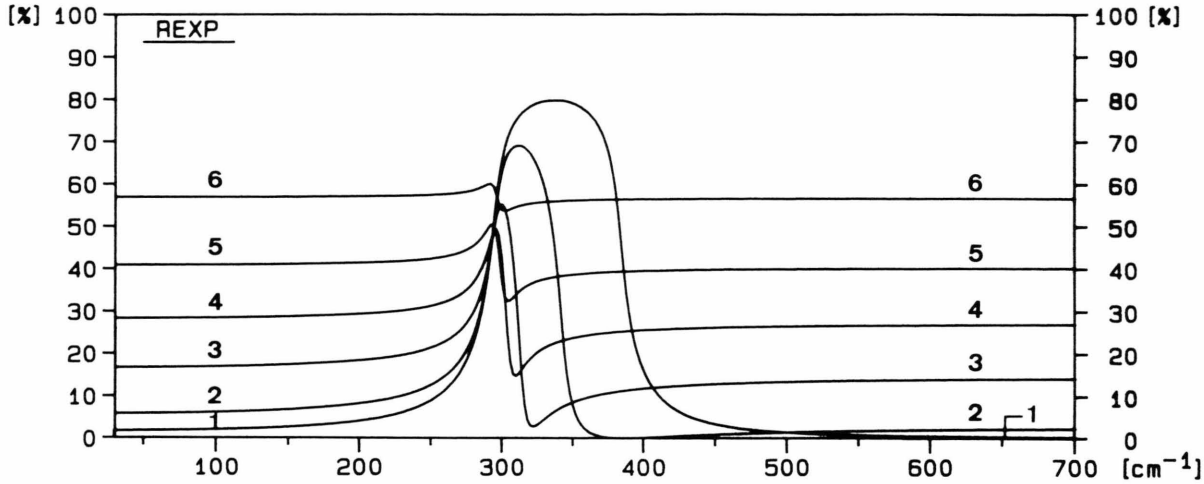

Fig. 7. Effect of the high-frequency dielectric constant ε_∞ on the shape of a reststrahlen band with oscillator strength being constant ($4\pi\varrho = 0.6895$, $\omega_{TO} = 295\ cm^{-1}$, $\gamma = 10\ cm^{-1}$) (1: $\varepsilon_\infty = 1$, $\omega_{LO} = 383.4\ cm^{-1}$, 6: 50, 297 cm^{-1}) [22].

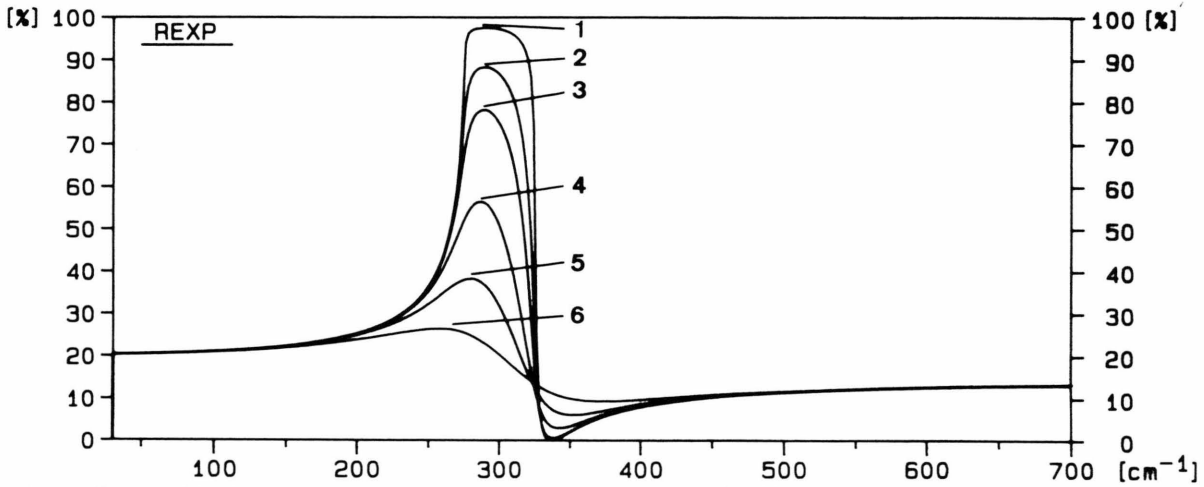

Fig. 8. Influence of the damping constant γ on the shape of reststrahlen bands with other oscillator parameters being constant ($\omega_{TO} = 275\ cm^{-1}$, $\omega_{LO} = 325\ cm^{-1}$, $\varepsilon_\infty = 5$) (1: $\gamma = 1\ cm^{-1}$, 6: $100\ cm^{-1}$) [22].

ω_{TO}, ω_{LO}, γ_{TO}, γ_{LO}, and ε_∞ are adjusted to the reflection spectra in a similar way as performed for the 3 PM. However, instead of the classical dielectric sum-function, the factorized form of the dielectric functions is used,

$$\hat{\varepsilon}_a(\omega) = \varepsilon_{\infty a} \prod_{f=1}^{m_a} \frac{\omega_{LOaf}^2 - i\gamma_{LOaf}\,\omega - \omega^2}{\omega_{TOaf}^2 - i\gamma_{TOaf}\,\omega - \omega^2}. \quad (12)$$

For details see [22].

The main advantages of the 4 parameter model are that (i) both ω_{TO} and ω_{LO} are directly obtained without use of dielectric dispersion functions – this allows to determine the LO frequencies of very weak reststrahlen bands –, (ii) fitting of the observed reflection spectra is easier than it is in the case of the 3 parameter model (see below), and (iii) different damping constants of the TO and LO phonons yield a better fit of the spectra. However, there are some restrictions with respect to the damping constants γ_{TO} and γ_{LO} [13], namely that

$$\gamma_{LOaf} \geq \gamma_{TOaf} \quad (13)$$

and

$$\gamma_{TOaf}/\gamma_{LOaf} \geq \omega_{TOaf}^2/\omega_{LOaf}^2. \quad (14)$$

A disadvantage of the 4 parameter model is that the oscillator strength of the phonons is not directly accessible. For details see [22].

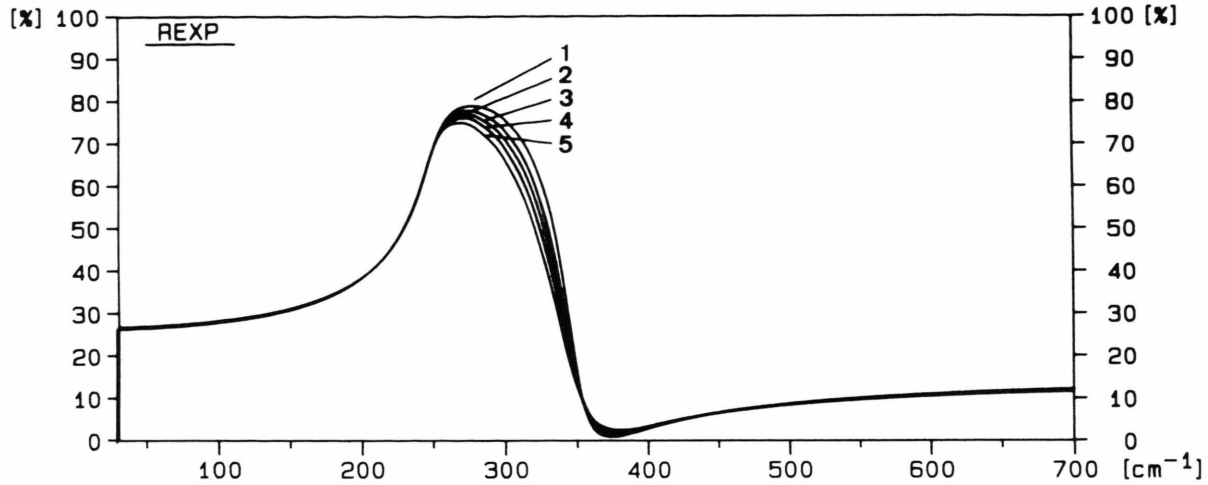

Fig. 9. Effect of increasing damping constant γ_{LO} on the shape of a reststrahlen band with γ_{TO} being constant ($\gamma_{TO} = 20\ cm^{-1}$, $\omega_{TO} = 250\ cm^{-1}$, $\omega_{LO} = 350\ cm^{-1}$, $\varepsilon_\infty = 5$) (1: $\gamma_{LO} = 20\ cm^{-1}$, 5: $40\ cm^{-1}$). Effect of γ_{TO} see [22].

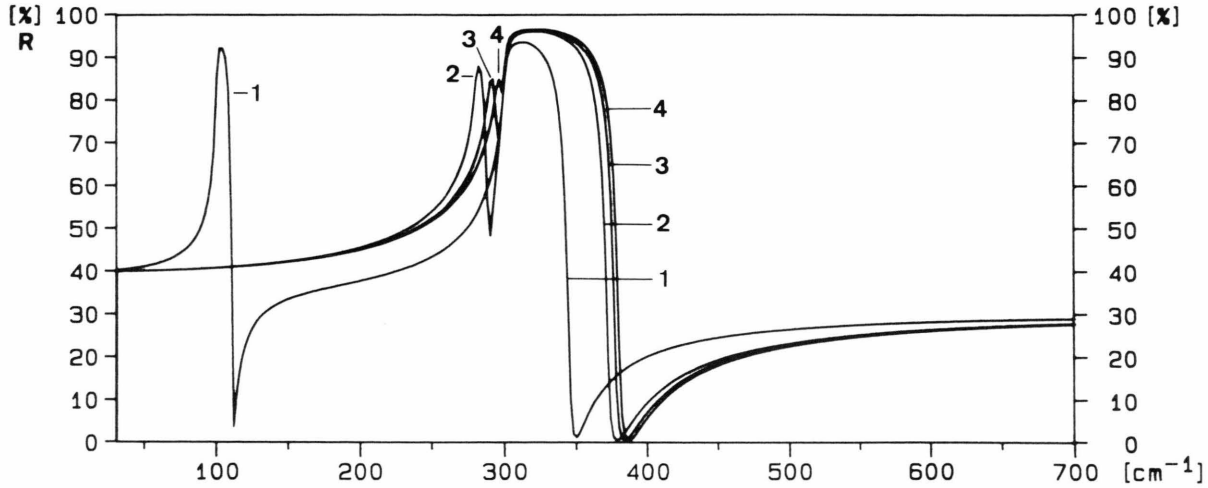

Fig. 10. Influence of the relative position of two oscillators on the shape of the reststrahlen bands ($4\pi\varrho = 3.8$, $\gamma = 0.012 \cdot \omega_{TO}\ cm^{-1}$, $\omega_{TO}(1) = 300\ cm^{-1}$) (1: $\omega_{TO}(2) = 100\ cm^{-1}$, 4: $295\ cm^{-1}$) [21].

6. Relevance of Oscillator Parameters – Model Calculations

The relevance of the various oscillator parameters to the reflection spectra in the presence of one phonon mode are illustrated in Figures 1–9. The main results are that (i) increase of both oscillator strength and TO/LO splitting (with the mean phonon energy being constant) greatly alters the intensity and shape of the reststrahlen bands (see Fig. 1) – this complicates fitting of the reststrahlen bands by 3 PM –, (ii) both the high-energy and the low-energy sides of a band remain unchanged if only ω_{TO} or ω_{LO} are changed, respectively (see Figs. 2 and 3) – this facilitates fitting of the reflection spectra using 4 PM –, (iii) a fixed TO/LO splitting results in the same band intensity irrespective of the spectral region chosen (see Figure 4), (iv) a fixed oscillator strength $4\pi\varrho$ produces different band intensities depending on the phonon frequency (see Fig. 5), (v) increase of the high-frequency dielectric constant ε_∞ changes the band shapes and intensities if the frequencies and the oscillator strength, respectively, are fixed (see Figs. 6 and 7), (vi) increasing damping constants flatten the reststrahlen bands (see Fig. 8), and (vii) the bands turn to an asymmetric shape if γ_{LO} is larger than γ_{TO} (see Fig. 9).

Model calculations of IR reflection spectra in the case of more than one reststrahlen band (see Fig. 10) and free carrier contributions are given in [21]. One of the results obtained is that in the case of adjoining reststrahlen bands (owing to the long-range electric-field coupling of LO phonons [21]) only the high-energy one produces a peak in the $-\mathrm{Im}(1/\hat{\varepsilon})(\omega)$ dispersion function (see below), i.e. ω_{LO} of the low-energy mode cannot be determined from the dielectric loss function. This phonon energy, however, is accessible using the 4 PM.

7. Determination of TO and LO Phonon Frequencies

The various methods of determining ω_{TO} and ω_{LO} reported in the literature (see Table 1) are based on the characteristics of transversal and longitudinal phonons. They yield equal mode energies if damping of the phonons can be neglected (and the high-frequency dielectric constant ε_∞ is not too large). In the case of large damping constants γ, the various methods do not result in consistent phonon frequencies. Some exemplary data calculated from $MnCr_2O_4$ single-crystal reflection spectra are shown in Table 2.

Thus, for example, the pole energies (maxima and minima) of the $|\hat{\varepsilon}|(\omega)$ dispersion function systematically deviate from those of the $\varepsilon''(\omega)$ and $-\mathrm{Im}(1/\hat{\varepsilon})(\omega)$ functions in such a manner that larger TO/LO splittings are obtained [16, 23]. These deviations are greater than 5 cm^{-1} in the case of broad, intense reststrahlen bands with large damping of the respective phonons and, hence, they cannot be neglected [22–24]. In the case of both large damping constants and high ε_∞ values, ω_{LO} cannot be derived from $\varepsilon'(\omega)$ because ε' does not turn to zero at ω_{LO}.

However, the oscillator parameters ω_{TO} (3 PM), and ω_{TO} and ω_{LO} (4 PM), and the phonon energies derived from the $\varepsilon''(\omega)$ and $-\mathrm{Im}(1/\hat{\varepsilon})(\omega)$ functions, respectively, commonly square within 2 cm^{-1} (irrespective of the evaluation procedures used) (see Table 2). These frequencies represent the true energies of the transversal and longitudinal optical phonon modes. This is also revealed from the findings that these parameters and pole energies coincide with the frequencies of the corresponding Raman scattering peaks observable in the case of solids which crystallize in non-centrosymmetric space groups [25, 26].

Therefore, in the case of Kramers-Kronig analyses and classical oscillator-fit calculations (3 PM), the pole energies of the imaginary part of both the dielectric constant $\varepsilon''(\omega)$ and the dielectric loss function $-\mathrm{Im}(1/\hat{\varepsilon})(\omega)$ should be used for determining the TO and LO phonon energies. Using the 4 parameter oscillator-fit model (4 PM), true TO and LO phonon energies can be obtained from the oscillator parameters ω_{TO} and ω_{LO}. However, in the case of broad asymmetric reststrahlen bands, reliable TO and LO phonon energies can only be obtained using 4 PM with different damping constants γ_{TO} and γ_{LO}.

Table 1. Procedures of determination of the TO and LO phonon frequencies from the poles (maxima, minima, and zero points 0) of the dispersion functions of the permittivities ε', ε'', and $|\hat{\varepsilon}|$ and the refractive index n.

ω_{TO}	ω_{LO}
max. $\varepsilon'(\omega)$ [a]	0 $\varepsilon'(\omega)$ [a]
max. $\varepsilon''(\omega)$ [b]	max. $-\mathrm{Im}(1/\hat{\varepsilon})(\omega)$ [c]
max. $\lvert\hat{\varepsilon}\rvert(\omega)$ [d]	min. $\lvert\hat{\varepsilon}\rvert(\omega)$ [d]
max. $n(\omega)$ [e]	min. $n(\omega)$ [e]

[a] Real part of the complex dielectric constant (permittivity) $\hat{\varepsilon}$, [b] Imaginary part of $\hat{\varepsilon}$, [c] Dielectric loss function, [d] Modulus (value) of $\hat{\varepsilon}$, [e] Refractive index.

Table 2. TO and LO phonon frequencies (cm^{-1}) of the zone-centre modes (species F_{1u}, unit-cell group O_h) of spinel-type $MnCr_2O_4$ obtained from IR single-crystal reflection spectra by various evaluation procedures (see Table 1). Reflection spectrum of a pressed pellet and data of other spinel-type oxides see [16].

	$\omega_{TO}^{(1)}$	$\omega_{TO}^{(2)}$	$\omega_{TO}^{(3)}$	$\omega_{TO}^{(4)}$	$\omega_{LO}^{(1)}$	$\omega_{LO}^{(2)}$	$\omega_{LO}^{(3)}$	$\omega_{LO}^{(4)}$
Kramers-Kronig analysis								
$\varepsilon'(\omega)$	186	365	473	597			543	695
$\lvert\hat{\varepsilon}\rvert(\omega)$	187	366	475	599	199	384	544	696
$n(\omega)$	186	366	474	598	199	384	521	671
$\varepsilon''(\omega)$	191	373	477	601				
$-\mathrm{Im}(1/\hat{\varepsilon})(\omega)$					195	379	543	695
Oscillator fit – 3 parameter model								
Oscillator-parameters	190.0	371.0	471.0	596.0				
$\varepsilon'(\omega)$	186	359	468	591			541	692
$\lvert\hat{\varepsilon}\rvert(\omega)$	187	363	471	595	196	387	541	692
$n(\omega)$	187	361	469	593	195	385	519	665
$\varepsilon''(\omega)$	190	371	471	596				
$-\mathrm{Im}(1/\hat{\varepsilon})(\omega)$					193	382	541	692
$4\pi\varrho$	0.02	0.07	0.2	0.06				
γ	7.8	25.6	5.7	8.9				
Oscillator fit – 4 parameter model								
Oscillator-parameters	190.0	370.5	467.5	595.5	193.2	380.0	541.8	690.5
$\varepsilon'(\omega)$	185	361	464	591			542	691
$\lvert\hat{\varepsilon}\rvert(\omega)$	187	364	467	595	197	386	542	691
$n(\omega)$	186	362	465	593	196	383	518	660
$\varepsilon''(\omega)$	190	371	468	595				
$-\mathrm{Im}(1/\hat{\varepsilon})(\omega)$					193	379	542	691
γ	9.1	22.5	6.0	8.7	9.2	22.6	8.0	11.6

The phonon frequencies obtained from single-crystal IR reflection spectra of spinel-type $MnCr_2O_4$ deviate up to 8 cm^{-1} from those obtained from spectra of pressed pellets (polycrystalline samples). See the discussion given in [16].

8. Conclusion and Recommendation

Among the three common procedures for evaluation of IR reflection spectra to determine reliable TO and LO phonon energies, the 4 parameter oscillator-fit method (4 PM) has several advantages. Thus, in the case of wide, asymmetric reststrahlen bands, only the 4 PM correctly describes the IR reflection spectra. On using ω_{TO}, ω_{LO}, γ_{TO}, and γ_{LO} as adjustable oscillator parameters (4 PM) it is much easier to fit reflection spectra than with 3 PM. Because approximate values of these oscillator parameters are available directly from the reflection spectra, only a few fitting steps are necessary. Using the 4 PM, true TO and LO phonon energies can be obtained directly from the oscillator parameters. No evaluation of the dispersion functions is required. However, if the number and approximate frequencies of the reststrahlen bands present are not known, Kramers-Kronig analysis is the only procedure which can be used.

[1] K. Huang, Proc. Roy. Soc. London **A 208,** 352 (1951).
[2] T. S. Robinson, Proc. Phys. Soc. London **B 65,** 910 (1952).
[3] F. Stern, Solid State Physics **15,** 299 (1963).
[4] C. K. Wu and G. Andermann, J. Opt. Soc. Amer. **58,** 519 (1968).
[5] D. M. Roessler, Brit. J. Appl. Phys. **17,** 1313 (1966).
[6] G. Andermann and D. A. Dows, J. Phys. Chem. Solids **28,** 1307 (1967).
[7] F. Abeles and I. P. Mathieu, Ann. Physique **3,** 5 (1961).
[8] W. G. Spitzer and D. A. Kleinman, Phys. Rev. **121,** 1324 (1961).
[9] T. S. Moss, Optical Properties of Semiconductors, Butterworths, London 1959.
[10] L. Merten, Z. Naturforsch. **22a,** 359 (1967), Phys. Stat. Sol. **30,** 449 (1968).
[11] L. Merten and G. Borstel, Z. Naturforsch. **27a,** 1792 (1972); J. Raman Spectrosc. **10,** 205 (1981).
[12] D. W. Berreman and F. C. Unterwald, Phys. Rev. **174,** 791 (1968).
[13] R. P. Lowndes, Phys. Rev. **B 1,** 2754 (1970).
[14] A. S. Chaves and S. P. S. Porto, Solid State Commun. **13,** 865 (1973).
[15] F. Gervais, Infrared and Millimeter Waves 8 (Ed. K. J. Button), New York 1983, p. 279–339.
[16] H. D. Lutz, B. Müller, and H. J. Steiner, J. Solid State Chem. **90,** 54 (1991).
[17] H. G. Häfele, in: H. Volkmann, Handbuch der Infrarotspektroskopie, Verlag Chemie, Weinheim 1972, p. 167–176.
[18] F. E. Volz, Appl. Opt. **22,** 1842 (1983).
[19] C. G. Olson and D. W. Lynch, Phys. Rev. **177,** 1231 (1969).
[20] H. D. Lutz, G. Schneider, and G. Kliche, J. Phys. Chem. Solids **46,** 437 (1985).
[21] G. Schneider, Thesis, Univ. Siegen (1983).
[22] J. Himmrich, Thesis, Univ. Siegen (1990).
[23] H. D. Lutz, G. Wäschenbach, G. Kliche, and H. Haeuseler, J. Solid State Chem. **48,** 196 (1983).
[24] K. Wussow, H. Haeuseler, P. Kuske, W. Schmidt, and H. D. Lutz, J. Solid State Chem. **78,** 117 (1989).
[25] A. S. Barker, Phys. Rev. **B 7,** 2507 (1979).
[26] M. Schmidt, Thesis, Universität Siegen 1992.